Published in final edited form as:

Cytokine. 2016 March ; 79: 12–22. doi:10.1016/j.cyto.2015.12.006.

Spatiotemporal phosphoprotein distribution and associated cytokine response of a traumatic injury

Alice A. Han[a,1], **Holly N. Currie**[a,1,2], **Matthew S. Loos**[b], **Julie A. Vrana**[a], **Emily B. Fabyanic**[a], **Maren S. Prediger**[a], **Jonathan W. Boyd**[a,*]

[a]C. Eugene Bennett Department of Chemistry, West Virginia University, Morgantown, WV, USA

[b]Department of Surgery, West Virginia University, Morgantown, WV, USA

Abstract

Molecular mechanisms of wound healing have been extensively characterized, providing a better understanding of the processes involved in wound repair and offering advances in treatment methods. Both spatial and temporal investigations of injury biomarkers have helped to pinpoint significant time points and locations during the recovery process, which may be vital in managing the injury and making the appropriate diagnosis. This study addresses spatial and temporal differences of phosphoproteins found in skeletal muscle tissue following a traumatic femur fracture, which were further compared to co-localized cytokine responses. In particular, several proteins (Akt, ERK, c-Jun, CREB, JNK, MEK1, and p38) and post-translational phosphorylations (p-Akt, p-c-Jun, p-CREB, p-ERK1/2, p-MEK1, p-p38, p-GSK3α/β, p-HSP27, p-p70S6K, and p-STAT3) associated with inflammation, new tissue formation, and remodeling were found to exhibit significant spatial and temporal differences in response to the traumatic injury. Quadratic discriminant analysis of all measured responses, including cytokine concentrations from previously published findings, was used to classify temporal and spatial observations at high predictive rates, further confirming that distinct spatiotemporal distributions for total protein, phosphorylation signaling, and cytokine (IL-1α, IL-1ß, IL2, IL6, TNF-α, and MIP-1α) responses exist. Finally, phosphoprotein measurements were found to be significantly correlated to cytokine concentrations, suggesting coordinated intracellular and extracellular activity during crucial periods of repair. This study represents a first attempt to monitor and assess integrated changes in extracellular and intracellular signaling in response to a traumatic injury in muscle tissues, which may provide a framework for future research to improve both our understanding of wounds and their treatment options.

Keywords

Spatiotemporal distribution; Phosphoprotein; Phosphorylation; Traumatic injury; Cytokine

*Corresponding author. Jonathan.Boyd@mail.wvu.edu (J.W. Boyd).
[1]Joint first authors.
[2]Present address: Department of Chemistry and Physics, California University of Pennsylvania, California, PA, USA.

1. Introduction

Wound healing in response to a traumatic injury is a highly complex process that is regulated by a myriad of coordinated biological processes and mechanisms. Conserved responses observed in wound repair have been classically characterized by three general stages: inflammation, new tissue formation, and remodeling [1]. While each stage serves a specific function and occurs at predictive time points, the healing process is described to transpire in continuous interdependent cellular and molecular steps that have not yet been fully elucidated [2]. Impairment of central steps, influenced by the severity and management of the wound, may delay repair or lead to additional detrimental risks, such as the development of non-viable tissue [3]. A heightened understanding of innate wound healing mechanisms offers opportunities to enhance medical treatments [4] and prevent further complications. Specifically, temporal and spatial changes of injury biomarkers are areas that have yet to be fully elucidated, but present prospective approaches to accelerate or aid in the recovery process. For example, progressive wound treatment strategies, such as tissue engineering, can be improved through the elucidation of spatial molecular patterns in injured tissue [5]. Additionally, standard techniques used to facilitate wound healing, such as surgical debridement [6] can be further refined through a better understanding of the spatiotemporal distribution of injury biomarkers. Determining the spatial aspect of repair may potentially aid surgeons to better determine which tissue to debride, while the temporal aspect of repair may help predict the outcome of injured tissue.

Most molecular level tissue injury response studies have focused on the time course of responses following injury, but the spatial aspect of molecular injury responses can also provide valuable insight for the understanding and treatment of traumatic wounds [7]. Several studies have reported various mechanistic features involved in healing: temporal and tissue dependent distributions of protein expression [8], temporal response of growth factors [9] and chemokines [10], and temporal and spatial responses of cytokines [11]. However, there has not yet been an investigation evaluating spatial and temporal phosphoprotein responses following a traumatic fracture injury. Protein phosphorylation is a fundamental and vital process centrally involved in many cellular processes that are intimately involved in the response to traumatic injury, including a role in the regulation of cell (and ultimately tissue) survival [12]. For instance, phosphorylation activity is notably involved in initiating cellular signaling cascades that are vital to all three stages of wound healing [13–15]. Thus, activation or deactivation of phosphoproteins, as well as fluctuations in phosphorylation levels, may describe cell signaling activity in states of cellular distress or different phases of recovery [16]. Examining phosphorylation changes under injured conditions lends a depiction of the healing process from a signaling aspect that may further advance the understanding and treatment of wounds.

Protein phosphorylation is a primary means by which extracellular signals, such as cytokines, are integrated within target cells, allowing cells to respond in a regulated manner and carry out the wound healing process. Phosphorylation levels observed in various severities of injury, ranging from traumatic brain injury [17] to dermal chemical burns [18], have been shown to exhibit distinct temporal response patterns. Certain phosphoproteins hold an especially central role in cell growth and survival, such as those within the mitogen-

activated protein kinase (MAPK) family. MAPK signaling is widely integrated in many processes responding to cellular distress. For instance, the involvement of increased MAPK signaling is becoming progressively prominent as a marker in many inflammatory diseases [19]. ERK1/2 [20], MEK [21], and JNK [22] are major components in the MAPK signaling pathway that have been described to significantly experience alterations during the repair process. Additionally, the coordination between MAPK pathway phosphorylation mediated signaling and other regulatory elements, such as growth factors, has been observed in cases of injury and wound healing [23].

In our previous research [11], we demonstrated a spatial cytokine distribution that exists following a Gustilo III-B [24] leg fracture in rats. As a continuation of that study, we have investigated the spatial and temporal intracellular phosphoprotein response in skeletal muscle tissue following traumatic injury. This study is the first to address measurable spatial and temporal differences of phosphoproteins found in muscle tissue following a traumatic injury severe enough to cause a bone fracture. Total levels of proteins in the MAPK family, along with an additional cohort of tightly associated downstream protein kinases, were measured in order to identify the differential distribution in response to the injury. Phosphorylation levels of proteins were also measured with an intention to further explore signaling activity during the recovery process. Spatial and temporal differences of all measured responses were statistically identified using ANOVA, and quadratic discriminant analysis was additionally used to classify temporal and spatial observations. Phosphoprotein responses measured in this study were also found to be related to previously published spatial and temporal cytokine responses [11]. Specifically, correlation analysis was conducted using total protein, phosphorylation, and previously published cytokine levels (measured from the same collected tissues) from Currie 2014, which for the first time allows a spatiotemporal examination of the coordinated relationship between cytokines and phosphoprotein (i.e. extracellular and intracellular) responses post traumatic injury. Overall, this research represents an alternative view of cellular response to a traumatic injury that offers an enhanced understanding of the underlying mechanisms that are involved in both initial response and repair.

2. Materials and methods

2.1. Animals

Adult male Sprague–Dawley rats were housed individually with a 12:12 light/dark cycle with ad libitum access to standard rat chow and water. Four time points were studied with 3 replicates each ($N = 3$) for a total of 12 rats for the study. All procedures were performed under the guidelines approved by the West Virginia University Animal Care and Use Committee.

2.2. Femur fracture

Buprenorphine SR was pre-operatively administered subcutaneously as an analgesic providing 72 h pain relief. Rats were anesthetized intraperitoneally with Ketamine (80–90 mg/kg) and Xylazine (10–15 mg/kg). This combination of analgesic and anesthetics has previously been identified as the best combination for avoiding significant modulation of

cytokine responses in a rat model [25]. Analgesics and anesthetics were additionally injected into the scruff on the back of the rat's neck. After administration of anesthesia, all animals were subjected to a standardized femur fracture on one leg using a custom designed tool in which a weight is dropped in a consistent fashion onto the mid-shaft of the rat's thigh [26]. This tool delivers a calculated force of 104.80 Newtons, generating a reproducible femur fracture and associated soft tissue injury. An incision was made to visualize the fracture to allow drilling of a hole into the proximal femur to allow a 0.045 in. Kirschner wire (K-wire) to be inserted down the intramedullary canal to fix the fracture. The incision was closed starting with the fascia, followed by a stainless steel suture on the skin. Rats were subcutaneously administered Yohimbine (2 mg/kg) post-operatively to reverse the Xylazine and were closely observed during recovery for signs of distress.

2.3. Sample preparation

Three rats were sacrificed at each of 4 time points (0, 6, 24, and 168 h post-fracture). It is crucial to understand that the $t = 0$ time point is not a true zero; instead, $t = 0$ represents the brief elapsed period of time between the occurrence of the traumatic injury and the collection of tissue samples. Rats were anesthetized intraperitoneally with Ketamine (80–90 mg/ kg) and Xylazine (10–15 mg/kg). One cc of Euthasol was then administered via intracardiac puncture. Skeletal muscle tissue was harvested from the following three locations: at the site of the fracture, 1.0 ± 0.2 cm away from the site of fracture, and from the leg opposite to the fractured leg [11]. Samples were immediately rinsed with ice cold phosphate buffered saline (PBS), snap frozen, and stored at −80 °C. Protein extraction was achieved using methods adapted from Hulse et al [27]. Samples were subsequently ground cryogenically and lyophilized. For analyses, 2–3 mg of lyophilized tissue sample was thawed for 10 min at 4 °C in cell lysis buffer (Bio-Rad, Hercules, CA) containing 20 mM phenylmethylsulfonyl fluoride (Sigma, St. Louis, MO). Thawed samples were then vortexed for 1–3 s and homogenized with 3 rapid pulses using an ultrasonic dismembrator. Following an additional 1–3 s of vortexing, samples were centrifuged at 5000g for 5 min at 4 °C. The supernatant was collected and total protein concentration was determined using the RCDC protein assay (Bio-Rad, Hercules, CA) according to the manufacturer's instructions. Absorbance values were determined using an Infinite M1000 plate reader (Tecan, Raleigh, NC).

2.4. Analyte measurement

Sample homogenates were diluted to a total protein concentration of 900 μg/ml with sample diluent (Bio-Rad, Hercules, CA). The relative abundance of total protein was determined using a Bio-plex kit containing polystyrene, non-magnetic antibody coated beads specific for Akt, c-Jun, CREB, ERK1/2, JNK, MEK1, and p38. Phosphoproteins were assayed using the Bio-plex phosphoprotein kit containing polystyrene, non-magnetic antibody coated beads specific for the following targets phosphorylated at the indicated amino acid residues: Akt (Ser472), c-Jun (Ser63), CREB (Ser133), ERK1/2 (Thr202/Tyr204, Thr185/Tyr187), JNK (Thr183/Tyr185), MEK1 (Ser217/ Ser221), p38 (Thr180/Tyr182), GSK-3α/ß (Ser21/Ser9), HSP27 (Ser78), IκBα (Ser536), p70S6K (Thr421/Ser424), and STAT3 (Tyr705). All beads were analyzed using the Bio-Plex 200 suspension array system, along with the Pro II Wash Station (Bio-Rad, Hercules, CA), according to the manufacturer's instructions.

2.5. Statistical analysis

Data were analyzed using Prism 5 (GraphPad, San Diego, CA) and SAS JMP (Carey, NC). Protein abundances were compared to a blank subtracted intensity of the relative fluorescence intensity (RFI) measured for each antibody-coated bead. Two-way analysis of variance (ANOVA) with Bonferroni's post-test was carried out using Prism 5, which identified significant differences ($p < 0.05$) between each sampling location and between time points. All measurements were performed in duplicate. Data are expressed as the mean ± standard error of the mean (SEM).

Quadratic discriminant analysis was conducted to evaluate the combined capacity of the protein, phosphoprotein, and cytokine responses [11] to predict the corresponding location and time of the injury. Using SAS JMP, all measured responses were cast as covariates (Y) and either location or time was assigned as the classification category (X); the *Shrink Covariances* option was applied to account for the different covariance within the categories. This analysis included 36 observations (3 rats for each of the 3 locations and 4 time points) for 25 different covariates. The mean of the covariates in a specific group was calculated, along with 95% confidence levels. Finally, biplot rays were determined that indicate how each covariate fits into the canonical space, with the direction signifying the degree of association within that space.

Significant pairwise correlations ($p < 0.05$) between cytokine and total protein/phosphoprotein responses were determined using SAS JMP. This analysis investigated the association of total protein levels and phosphorylation responses with cytokine production at each time point and sample location. Data used for spatial correlation analysis consisted of values from every time point (0, 6, 24, and 168 h), with a maximum N of 12. Data used for temporal analysis included values from all sample locations (At fracture, 1-cm away, and uninjured leg), with a maximum N of 9. Outliers, or data points that were driving the correlation were identified and eliminated using boundaries set by the interquartile range.

3. Results

3.1. Spatial and temporal total protein levels

Relative levels of total protein, regardless of the phosphorylation state (phosphorylated or unphosphorylated) are presented in Fig. 1 for 7 targets: Akt, c-Jun, CREB, ERK1/2, JNK, MEK1, and p38. Immediately following injury (at hour 0), total Akt and ERK1/2 levels were significantly higher ($p < 0.05$) in tissue taken from the uninjured leg in comparison to tissue at the fracture site and to the tissue sampled 1-cm away from the fracture. No other proteins exhibited significant differences among the three sample sites at hour 0. At 6 h post-fracture, expression of only p38 was significantly different at the fracture site compared to the amount found in the uninjured tissue. Spatial variances in p38 expression continued to persist at 24 h post-fracture, when the level at the fracture site was significantly lower than levels found in both 1-cm away and uninjured tissue samples. MEK1 was additionally observed to exhibit a spatial gradient 24 h after injury, with significantly lower levels at the fracture site compared to tissue 1-cm away and in the uninjured leg.

The highest number of significant differences in protein expression among different sampling locations was observed 168 h post-fracture. Expression levels of Akt and ERK1/2 were significantly higher at the site of injury in comparison to the uninjured leg, while c-Jun, CREB, JNK, and p38 levels were all statistically higher at the site of fracture in comparison to both 1-cm away and uninjured tissue samples. It was noted that the spatial pattern observed at 168 h was opposite the trend observed at the earlier time points, with protein expression levels being highest at the site of fracture.

3.2. Spatial and temporal response of phosphorylated proteins

To further examine the contribution of the selected proteins, phosphorylation levels were determined for the following targets: Akt, c-Jun, CREB, ERK1/2, JNK, MEK1, p38 (Fig. 2). In addition, phosphorylation responses of GSK-3α/ß, HSP27, IκBα, p70S6K, and STAT3 (Fig. 3) were also measured. No statistically significant spatial differences for phosphorylated JNK or IκBα were observed at any time point. At 0 h post-fracture, phosphorylated levels of Akt, c-Jun, ERK1/2, GSK-3α/ß, HSP27, p70S6K, and STAT3 were significantly higher in tissue taken from the uninjured leg compared to both tissue samples collected at the fracture site and 1-cm away from the fracture. In contrast, CREB phosphorylation levels only differed between the uninjured and 1-cm away site, while phosphorylation of MEK1 and p38 did not present any spatial differences.

At the later time points, the number of phosphorylated proteins with significant spatial differences decreased. Only Akt, GSK-3α/ß, and MEK1 displayed spatial gradients at 6 h post-fracture, with the lowest degree of phosphorylation at the site of fracture for Akt and GSK-3α/ß. At 24 h post-fracture, GSK-3α/ß continued to present spatial phosphorylation differences, along with a newly present p38. Phosphorylation levels of both GSK-3α/ß and p38 were lowest at the site of fracture during this time. The distribution of phosphorylated proteins at the final time point (168 h) deviated from the pattern observed at the earlier times. While most of the gradients revealed lower levels of phosphorylated protein at the fracture site at 0, 6, and 24 h, the levels of phosphorylated MEK1 and p70S6K were highest at the site of tissue injury at 168 hours post-fracture.

3.3. Spatial and temporal cytokine concentrations

Fig. 4 shows an adapted figure from Currie, et al. demonstrating spatial and temporal differences of cytokine responses following the same traumatic injury as described in this paper [11]. Concentrations of the following cytokines were measured: IL-1α, IL-1ß, IL2, IL6, TNF-α, and MIP-1α. IL-2 was the sole cytokine with any spatial differences at $t = 0$, but did not exhibit any significant differences at the other time points. IL-1ß and IL6 displayed strong significant changes in spatial response only at $t = 6$, while IL-1α represented the single cytokine to express spatial alterations at $t = 24$. TNF-α, and MIP-1α did not exhibit any statistically significant spatial nor temporal differences.

3.4. Quadratic to discriminant analysis used predict location and of time injury

Quadratic discriminant analysis was performed using all measured responses: total protein concentration (Akt, c-Jun, CREB, ERK1/2, JNK, MEK1, p38), phosphorylation levels (p-Akt, p-c-Jun, p-CREB, p-ERK1/2, p-JNK, p-MEK1, p-p38, p-GSK-3α/ß, p-HSP27, p-

IκBα, p-p70S6K, and p-STAT3), and cytokine concentrations determined in a previous study (IL-1α, IL-1ß, IL2, IL6, TNF-α, and MIP-1α) [11]. This analysis classified the combined observed responses into pre-determined groups (location or time) by plotting each collective observation against two canonical coordinates. In Figs. 5 and 6, the location and time of injury were predicted based on the responses associated with each sample, respectively. In total, discriminant analysis misclassified only 10 observations out of 36 for location predictions and none for time predictions: 4 observations that were derived from samples taken from the site of injury were predicted as belonging to the 1-cm away group and 6 observations that were associated with samples from the other uninjured leg were incorrectly grouped in the 1-cm away group.

3.5. Correlation between and cytokine phosphoprotein response

The results of the correlation analysis between protein and phosphorylation responses in this study (Akt, c-Jun, CREB, ERK1/2, JNK, MEK1, p38, GSK-3α/ß, HSP27, IκBα, p70S6K, and STAT3) and cytokine responses from a previous study (IL-1α, IL-1ß, IL2, IL6, TNF-α, and MIP-1α) [11] are presented in Tables 1–4. The responses were compared across the three locations and at each of the four time points. It is important to note that these correlations are possible because the tissue samples are from the same animals, locations, and time points as described in Currie, 2014. Significant spatial correlations (Tables 1 and 2) identified certain cytokines and phosphoproteins that responded similarly at particular locations. At the site of the fracture, MIP-1α was a noted contributor with negative correlations to four proteins (CREB, MEK, c-Jun, and Akt) and phosphorylation responses of five phosphoproteins (Akt, p70S6K, GSK-3α/ß, MEK1, and ERK1/2). Although there were no statistically significant spatial nor temporal differences for MIP-1α, a general decrease in concentration can be seen with increasing time. Moving 1-cm away from the site of injury, IL2 and IL-1ß joined MIP-1α in being negatively correlated to a larger collection of proteins and phosphoproteins with the exception of two positive correlations between IL2/IκBα and IL-1ß/STAT3 (Table 2). More positive correlations were identified in the sample from the uninjured leg: MEK1 levels were negatively correlated to cytokines IL6 and IL2 measured in the uninjured leg, while Akt levels were positively correlated to one cytokine (IL-1α). All positive correlations between phosphorylation and cytokine responses (IL2/STAT3, IL2/JNK, TNF-α/ERK1/2, TNF-α/p70S6K) were also found in the uninjured leg.

Temporal correlation analysis between total protein and cytokine levels (Table 3) identified eight significant pairs at 0 hours post fracture (IL6/p38, IL6/c-Jun, IL6/MEK1, IL-1α/c-Jun, TNF-α/p38, IL2/p38, IL2/MEK1, and MIP-1α/c-Jun), six pairs at 6 hours post fracture (IL6/p38, IL6/ERK1/2, IL6/JNK, IL-1ß/p38, IL-1ß/JNK, and IL-1ß/ERK1/2), and no correlations at 24 and 168 hours post fracture. Temporal correlation analysis between cytokine and phosphoprotein responses (Table 4) determined five pairwise correlations at 0 hours post-fracture (IL-1α/GSK-3α/ß, IL-1α/p70S6K, IL6/CREB, IL2/CREB, and IL2/MEK1), three correlations at 6 h (IL-1α/c-Jun, IL-1ß/JNK, and MIP-1α/Akt), three correlations at 24 h (IL6/HSP27, IL6/CREB, and IL-1ß/HSP27), and zero correlations at 168 h. All correlations between protein and cytokine levels were negative, while a mixture of positive and negative correlations was identified for phosphorylation and cytokine responses.

4. Discussion

Spatial and temporal differences in phosphorylation mediated signaling in response to a traumatic injury is still an unfamiliar area within the field of wound healing mechanisms. Injury and repair biomarkers, including cytokines, neutrophils, leukocytes, and growth factors are some of the more characterized aspects, but piecing all of the components together is a necessity to improve our understanding of the wound healing process. This study provides a depiction of the intracellular signaling that occurs as a result of a reproducible leg fracture model, in an effort to deliver an enhanced understanding of the healing process and treatment options. Defining location and time dependent differences in phosphoprotein response, along with identifying associations with cytokine production, was the focus of this investigation.

Measurement of the total protein levels (phosphorylated and unphosphorylated) identified several proteins with a suggested significance at certain time points and locations (Fig. 1). In particular, a differential distribution of Akt and ERK protein expression at the different sampling locations was observed. Akt and ERK1/2 pathways are notably recognized as key contributors of cell growth and survival [28,29] and the data in this study demonstrated that they become more active, through increased expression, during the later stages in the healing process when new tissue formation and remodeling is likely to occur. Other proteins (c-Jun, CREB, JNK, MEK1, and p38) also exhibited significant spatial differences at later time points. In agreement with previous studies, MAPK signaling pathways involving ERK1/2, MEK1, and JNK have been reported to respond to injuries induced in skeletal muscles [30].

While assessing protein expression can offer substantial insight into the healing mechanism, it is necessary to evaluate the associated post-translational activity since alterations in protein abundance are not as immediate as phosphorylation processes. All of the measured total proteins were evaluated for phosphorylation responses, and in an effort to investigate a larger collection of phosphorylation changes, GSK-3α/ß, HSP27, IκBα, p70S6K, and STAT3 were also monitored (Figs. 2 and 3). Similar to the response of total protein expression, the results indicate that protein phosphorylation at early time points (0 and 6 h post injury) is generally decreased at the fracture site and surrounding regions, as there were no instances where phosphorylated protein levels were lower in the uninjured tissue. This decrease in phosphorylation may be due to a combination of increased apoptosis [31], decreased cellular regulation over kinase activity [32], injury induced hypoxia [33] and, in contrast, hyperoxia [34], or ATP availability [35]. For proteins that experienced increases in phosphorylation at or near the site of fracture, this typically occurred at the later time points, suggesting prominent roles for these proteins in the later stages of mediating repair. It is important to note that a decreased level in phosphorylation does not necessarily equate to a decrease in activity of that protein. For instance, a decrease in Ser-21/9 phosphorylation on GSK-3α/ß corresponds to an increase in GSK-3α/ß activity [36]. Two of the measured phosphoproteins, JNK and IκBα, did not exhibit temporal or spatial differences in phosphorylation, but this is only true at the specific time points selected in this study.

In order to begin to understand the integrated cellular response to traumatic injury and follow-on wound healing, it is also useful to examine the relationships and coordinated

efforts of related proteins. For example p70S6K is implicated as a downstream target of the Akt/mammalian target of rapamycin (mTOR) signaling pathway following its activation during muscle remodeling [37]. The Akt signaling pathway is also known to promote protein synthesis to increase muscle mass through the activation of p70S6K [38]. In agreement with these previous studies, this work shows that at the last time point measured (168 h post-fracture), at the site of fracture, the phosphorylation levels of Akt had increased and returned to comparable levels as found in the uninjured leg. At the same time, phosphorylation levels of p70S6K were also significantly amplified at the site of fracture, indicating the increased phosphorylation levels of both proteins may signify crucial times of muscle repair. GSK-3α/ß, another downstream target of the Akt signaling pathway, is known to be an extremely important mediator of muscle tissue plasticity, and has been observed to increase in activity in skeletal muscle resulted from burn injuries [39]. Akt inhibits GSK-3α/ß activity directly by phosphorylating Ser-21 and Ser-9 on the α and ß isoforms, respectively [40]. At the 0 time point, Akt protein expression and phosphorylation along with GSK-3α/ß phosphorylation seemed to be in accord, with significantly lower levels at the fracture site in comparison to the uninjured leg. These results suggest GSK-3α/ß phosphorylation is associated with Akt during early periods after the fracture.

One of the most well characterized aspects of the response to traumatic injury is the regulatory role of cytokines. Cytokine production has been shown to reflect the degree of tissue trauma, and temporal changes in cytokine concentrations have been shown to correlate with adverse early post-trauma implications such as acute respiratory distress syndrome (ARDS) [41], multiple organ failure (MOF) [42], and mortality [43]. In previous studies, correlations between repair biomarkers and phosphoprotein responses have been identified. For instance, the degree of GSK-3α/ß phosphorylation is reported to be strongly correlated to levels of β-catenin protein, a crucial regulator of wound healing [44]. p38 is also known to respond to cytokines and various types of stress [45] and has been shown to increase dramatically in injured human muscle [46]. In the context of wound healing, cytokine expression and phosphorylation levels of associated proteins have been linked together [47], implicating the importance of integrated extracellular and intracellular signaling during crucial periods of repair. Cytokine responses (Fig. 4) from previous research also exhibited a spatiotemporal distribution as a result of the same traumatic injury. In this study, discriminant analysis was conducted using protein, phosphorylation, and cytokine levels in order to evaluate all three responses, collectively, for all locations and time points. Correlation analysis was also performed to investigate the pairwise spatiotemporal relationships among total protein, phosphoproteins, and cytokines.

Discriminant analysis has previously been demonstrated to successfully predict adverse outcomes, such as ligament injuries [48], cardiotoxicity [49], and asphyxia [50]. Instead of predicting adverse outcomes, the observed responses reported in this study were used to distinguish between different locations and times of injury (Figs. 5 and 6). Classification of the observations based on time yielded a prediction rate of 100%, while classification based on location yielded a prediction rate of about 72%, incorrectly placing 10 out of 36 observations into the wrong groups. The misclassified observations only occurred for location predictions: 4 observations from the site of injury group were predicted as belonging to the 1-cm away group and 6 observations from other uninjured leg group were

incorrectly grouped in the 1-cm away group. These misclassifications were not unexpected because although the 1-cm away samples are technically uninjured tissue, the surrounding area near the site of injury still experienced indirect impacts (i.e. inflammation) from the traumatic injury. These results indicate that there is a strong temporal and spatial distinction in tissue response following a traumatic injury that can be observed with both intracellular (total protein, phosphorylation) and extracellular (cytokine) responses, further confirming that a distinct spatiotemporal gradient for all three responses exist. The promising predictive rates also suggest a coordinated effort of proteins, phosphorylation signaling, and cytokine regulation in response to the injury since each observation (data point in the canonical plot) integrated all measurements of the dataset.

Finally, significant correlated pairings of phosphoprotein and cytokine responses were discerned (Tables 1–4) in order to monitor how associated pairs may be altered over time and location. As a primary marker of injury, cytokines may be critical for initiating certain processes, such as protein expression or phosphorylation, especially in cases of traumatic tissue injury. The absence and/or development of correlations may be indicative of the progression of the healing process, or lack thereof. For instance, all correlations between total protein and cytokines were negative at the two early time points, suggesting some form of ordered regulation. After 6 h, zero correlations were observed, indicating a drastic change in cytokine production, protein expression, or both. While these results offer a glimpse of the tightly coordinated signaling efforts at distinct phases of repair, we believe that a more comprehensive modeling effort of spatiotemporal responses should be undertaken in order to improve our understanding of this fundamental process.

5. Conclusions

The vast majority of studies investigating the specific roles of proteins under injurious inflammatory inducing conditions are performed in vitro, typically focusing on the up or down regulation of a few select proteins. The results presented here are unique in that they reflect the entire tissue response to trauma. Overall, the data indicate that there are observable significant spatial differences in the levels of phosphorylated proteins following a traumatic injury. This is the first study to analyze the levels of phosphorylated proteins in tissue samples at different distances from a traumatic injury. It provides evidence that monitoring phosphoproteins could potentially be used to spatially assess the state of injured tissue. Additionally, exploring the integration of phosphoprotein and cytokine signaling roles under conditions of distress offers insight into the healing mechanism. This information may potentially be helpful in adapting or refining wound treatment procedures, such as the debridement of non-viable tissue, in order to prevent additional adverse outcomes resulting from possible treatment complications.

Acknowledgements

This research was conducted with support from a grant awarded by The Brodie Discovery and Innovation Fund.

References

[1]. Gurtner GC, Werner S, Barrandon Y, Longaker MT, Wound repair and regeneration, Nature 453 (2008) 314–321. [PubMed: 18480812]

[2]. Velnar T, Bailey T, Smrkoli V, The wound healing process: an overview of the cellular and molecular mechanisms, J. Int. Med. Res 37 (2009) 1528–1542. [PubMed: 19930861]

[3]. Witte MB, Barbul A, General principles of wound healing, Surg. Clin. North Am (1997) 77. 509-+.

[4]. Broughton G 2nd, Janis JE, Attinger CE, The basic science of wound healing, Plast. Reconstr. Surg 117 (2006) 12s–34s. [PubMed: 16799372]

[5]. Lee K, Silva EA, Mooney DJ, Growth factor delivery-based tissue engineering: general approaches and a review of recent developments, J R Soc. Interf 8 (2011) 153–170.

[6]. Akita S, Surgical debridement, in: Skin Necrosis, Springer, Vienna, 2015, pp. 257–263.

[7]. Gerstenfeld LC, Cullinane DM, Barnes GL, Graves DT, Einhorn TA, Fracture healing as a post-natal developmental process: molecular, spatial, and temporal aspects of its regulation, J. Cell Biochem 88 (2003) 873–884. [PubMed: 12616527]

[8]. Rittie L, Perbal B, Castellot JJ Jr., Orringer JS, Voorhees JJ, Fisher GJ, Spatial-temporal modulation of CCN proteins during wound healing in human skin in vivo, J. Cell Commun. signaling. 5 (2011) 69–80.

[9]. Kibe Y, Takenaka H, Kishimoto S, Spatial and temporal expression of basic fibroblast growth factor protein during wound healing of rat skin, Br. J. Dermatol 143 (2000) 720–727. [PubMed: 11069447]

[10]. Gillitzer R, Goebeler M, Chemokines in cutaneous wound healing, J. Leukoc. Biol 69 (2001) 513–521. [PubMed: 11310836]

[11]. Currie HN, Loos MS, Vrana JA, Dragan K, Boyd JW, Spatial cytokine distribution following traumatic injury, Cytokine 66 (2014) 112–118. [PubMed: 24461742]

[12]. Hunter T, Protein kinases and phosphatases: the yin and yang of protein phosphorylation and signaling, Cell 80 (1995) 225–236. [PubMed: 7834742]

[13]. Viatour P, Merville MP, Bours V, Chariot A, Phosphorylation of NF-kappaB and IkappaB proteins: implications in cancer and inflammation, Trends Biochem. Sci 30 (2005) 43–52. [PubMed: 15653325]

[14]. Payne J, Gong H, Trinkaus-Randall V, Tyrosine phosphorylation: a critical component in the formation of hemidesmosomes, Cell Tissue Res. 300 (2000) 401–411. [PubMed: 10928271]

[15]. Kasza KE, Farrell DL, Zallen JA, Spatiotemporal control of epithelial remodeling by regulated myosin phosphorylation, Proc. Natl. Acad. Sci. USA 111 (2014) 11732–11737.

[16]. Richards TS, Dunn CA, Carter WG, Usui ML, Olerud JE, Lampe PD, Protein kinase C spatially and temporally regulates gap junctional communication during human wound repair via phosphorylation of connexin43 on serine368, J. Cell Biol 167 (2004) 555–562. [PubMed: 15534005]

[17]. Noshita N, Lewen A, Sugawara T, Chan PH, Akt phosphorylation and neuronal survival after traumatic brain injury in mice, Neurobiol. Dis 9 (2002) 294–304. [PubMed: 11950275]

[18]. Rebholz B, Kehe K, Ruzicka T, Rupec RA, Role of NF-kappaB/RelA and MAPK pathways in keratinocytes in response to sulfur mustard, J. Invest. Dermatol 128 (2008) 1626–1632. [PubMed: 18200059]

[19]. Kaminska B, MAPK signalling pathways as molecular targets for anti-inflammatory therapy-from molecular mechanisms to therapeutic benefits, Biochim. Biophys. Acta 1754 (2005) 253–262. [PubMed: 16198162]

[20]. Sharma GD, He J, Bazan HE, P38 and ERK1/2 coordinate cellular migration and proliferation in epithelial wound healing: evidence of cross-talk activation between MAP kinase cascades, J. Biol. Chem 278 (2003) 21989–21997.

[21]. Seah CC, Phillips TJ, Howard CE, Panova IP, Hayes CM, Asandra AS, et al., Chronic wound fluid suppresses proliferation of dermal fibroblasts through a Ras-mediated signaling pathway, J. Invest. Dermatol 124 (2005) 466–474. [PubMed: 15675969]

[22]. Ramet M, Lanot R, Zachary D, Manfruelli P, JNK signaling pathway is required for efficient wound healing in Drosophila, Dev. Biol 241 (2002) 145–156. [PubMed: 11784101]

[23]. Huh JE, Nam DW, Baek YH, Kang JW, Park DS, Choi DY, et al., Formononetin accelerates wound repair by the regulation of early growth response factor-1 transcription factor through the phosphorylation of the ERK and p38 MAPK pathways, Int. Immunopharmacol 11 (2011) 46–54. [PubMed: 20959155]

[24]. Gustilo RB, Mendoza RM, Williams DN, Problems in the management of type III (severe) open fractures: a new classification of type III open fractures, J. Trauma 24 (1984) 742–746. [PubMed: 6471139]

[25]. Al-Mousawi AM, Kulp GA, Branski LK, Kraft R, Mecott GA, Williams FN, et al., Impact of anesthesia, analgesia, and euthanasia technique on the inflammatory cytokine profile in a rodent model of severe burn injury, Shock 34 (2010) 261–268. [PubMed: 20803788]

[26]. Lindsey BA, Clovis NB, Smith ES, Salihu S, Hubbard DF, An animal model for open femur fracture and osteomyelitis–Part II: immunomodulation with systemic IL-12, J. Orthop. Res 28 (2010) 43–47. [PubMed: 19623664]

[27]. Hulse RE, Kunkler PE, Fedynyshyn JP, Kraig RP, Optimization of multiplexed bead-based cytokine immunoassays for rat serum and brain tissue, J. Neurosci. Meth 136 (2004) 87–98.

[28]. Song G, Ouyang G, Bao S, The activation of Akt/PKB signaling pathway and cell survival, J. Cell Mol. Med 9 (2005) 59–71. [PubMed: 15784165]

[29]. Mebratu Y, Tesfaigzi Y, How ERK1/2 activation controls cell proliferation and cell death: is subcellular localization the answer?, Cell Cycle 8 (2009) 1168–1175 [PubMed: 19282669]

[30]. Yeow K, Cabane C, Turchi L, Ponzio G, Derijard B, Increased MAPK signaling during in vitro muscle wounding, Biochem. Biophys. Res. Commun 293 (2002) 112–119. [PubMed: 12054571]

[31]. Keshavjee S, Zhang XM, Fischer S, Liu M, Ischemia reperfusion-induced dynamic changes of protein tyrosine phosphorylation during human lung transplantation, Transplantation 70 (2000) 525–531. [PubMed: 10949198]

[32]. Irving EA, Bamford M, Role of mitogen-and stress-activated kinases in ischemic injury, J. Cereb. Blood. Flow Metab 22 (2002) 631–647. [PubMed: 12045661]

[33]. Tandara AA, Mustoe TA, Oxygen in wound healing–more than a nutrient, World J. Surg 28 (2004) 294–300. [PubMed: 14961188]

[34]. Sen CK, Wound healing essentials: let there be oxygen, Wound Repair Regen. 17 (2009) 1–18. [PubMed: 19152646]

[35]. Chiang B, Essick E, Ehringer W, Murphree S, Hauck MA, Li M, et al., Enhancing skin wound healing by direct delivery of intracellular adenosine triphosphate, Am. J. Surg 193 (2007) 213–218. [PubMed: 17236849]

[36]. Jope RS, Johnson GV, The glamour and gloom of glycogen synthase kinase-3, Trends. Biochem. Sci 29 (2004) 95–102. [PubMed: 15102436]

[37]. Bassel-Duby R, Olson EN, Signaling pathways in skeletal muscle remodeling, Annu. Rev. Biochem 75 (2006) 19–37. [PubMed: 16756483]

[38]. Guttridge DC, Signaling pathways weigh in on decisions to make or break skeletal muscle, Curr. Opin. Clin. Nutr. Metab. Care 7 (2004) 443–450. [PubMed: 15192448]

[39]. Fang CH, Li B, James JH, Yahya A, Kadeer N, Guo X, et al., GSK-3beta activity is increased in skeletal muscle after burn injury in rats, Am. J. Physiol. Regul. Integr. Comp. Physiol 293 (2007) R1545–R1551.

[40]. Moore SF, van den Bosch MT, Hunter RW, Sakamoto K, Poole AW, Hers I, Dual regulation of glycogen synthase kinase 3 (GSK3)alpha/beta by protein kinase C (PKC)alpha and Akt promotes thrombin-mediated integrin alphaIIbbeta3 activation and granule secretion in platelets, J. Biol. Chem 288 (2013) 3918–3928. [PubMed: 23239877]

[41]. Park WY, Goodman RB, Steinberg KP, Ruzinski JT, Radella F 2nd, Park DR, et al., Cytokine balance in the lungs of patients with acute respiratory distress syndrome, Am. J. Respir. Crit. Care Med 164 (2001) 1896–1903. [PubMed: 11734443]

[42]. Maier B, Lefering R, Lehnert M, Laurer HL, Steudel WI, Neugebauer EA, et al., Early versus late onset of multiple organ failure is associated with differing patterns of plasma cytokine

biomarker expression and outcome after severe trauma, Shock 28 (2007) 668–674. [PubMed: 18092384]

[43]. Simmons EM, Himmelfarb J, Sezer MT, Chertow GM, Mehta RL, Paganini EP, et al., Plasma cytokine levels predict mortality in patients with acute renal failure, Kidney Int. 65 (2004) 1357–1365. [PubMed: 15086475]

[44]. Cheon SS, Nadesan P, Poon R, Alman BA, Growth factors regulate beta-catenin-mediated TCF-dependent transcriptional activation in fibroblasts during the proliferative phase of wound healing, Exp. Cell Res 293 (2004) 267–274. [PubMed: 14729464]

[45]. Cargnello M, Roux PP, Activation and function of the MAPKs and their substrates, the MAPK-activated protein kinases, Microbiol. Mol. Biol. Rev 75 (2011) 50–83. [PubMed: 21372320]

[46]. Aronson D, Wojtaszewski JF, Thorell A, Nygren J, Zangen D, Richter EA, et al., Extracellular-regulated protein kinase cascades are activated in response to injury in human skeletal muscle, Am. J. Physiol 275 (1998) C555–C561. [PubMed: 9688610]

[47]. Ishida Y, Kondo T, Takayasu T, Iwakura Y, Mukaida N, The essential involvement of cross-talk between IFN-gamma and TGF-beta in the skin wound-healing process, J. Immunol 172 (2004) 1848–1855. [PubMed: 14734769]

[48]. Simon RA, Everhart JS, Nagaraja HN, Chaudhari AM, A case-control study of anterior cruciate ligament volume, tibial plateau slopes and intercondylar notch dimensions in ACL-injured knees, J. Biomech 43 (2010) 1702–1707. [PubMed: 20385387]

[49]. Li Y, Ju L, Hou Z, Deng H, Zhang Z, Wang L, et al., Screening, verification, and optimization of biomarkers for early prediction of cardiotoxicity based on metabolomics, J. Proteome. Res 14 (2015) 2437–2445. [PubMed: 25919346]

[50]. Longini M, Giglio S, Perrone S, Vivi A, Tassini M, Fanos V, et al., Proton nuclear magnetic resonance spectroscopy of urine samples in preterm asphyctic newborn: a metabolomic approach, Clin. Chim. Acta 444 (2015) 250–256. [PubMed: 25727514]

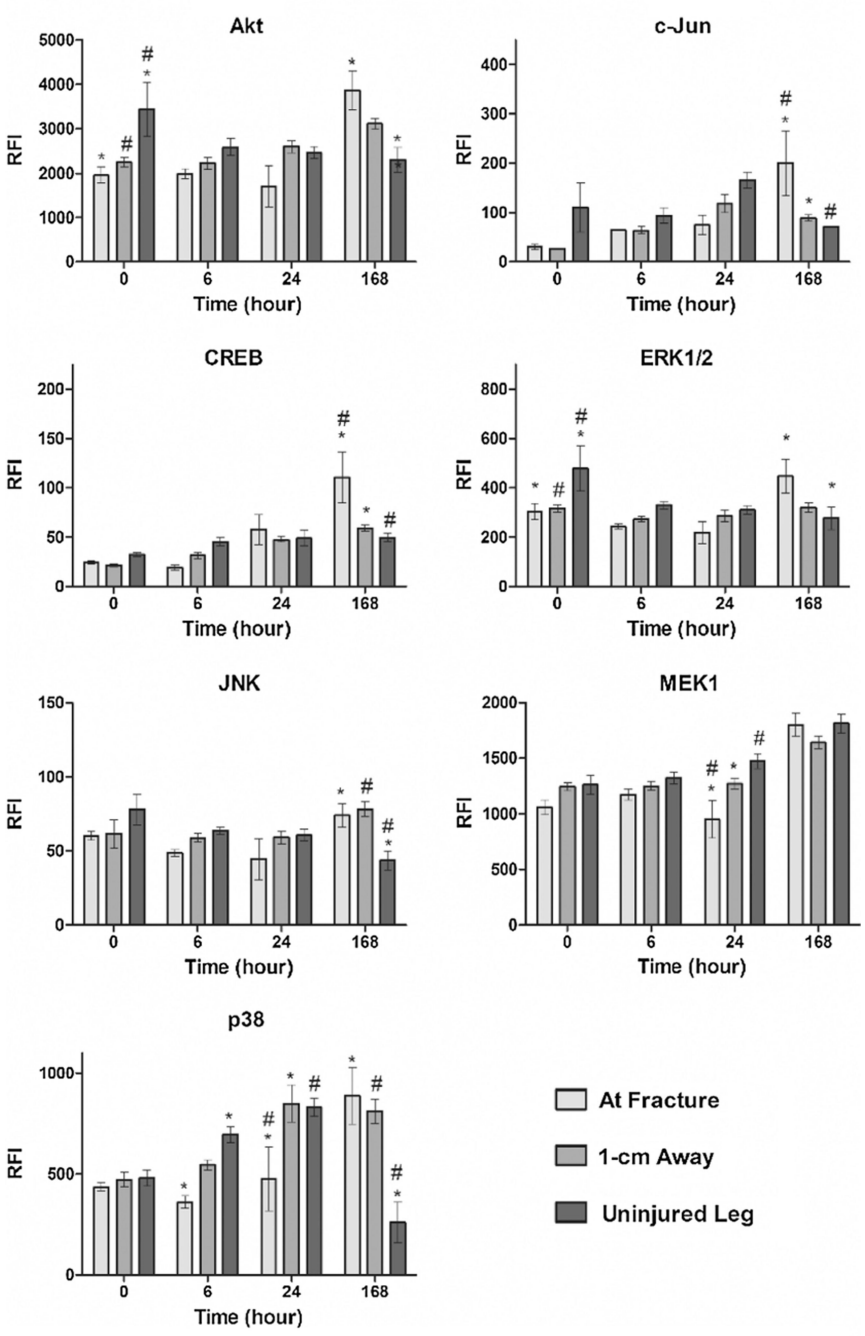

Fig. 1.

Total protein concentration measured across time and location in response to a traumatic injury. Relative fluorescence intensity (RFI) associated with total protein concentrations of the following proteins were assayed across four time points and three different locations following the femur fracture: Akt, c-Jun, CREB, ERK1/2, JNK, MEK1, and p38. Statistically significant differences ($p < 0.05$) in protein concentration between different locations are marked with matching symbols (* or #). Error bars reflect ± standard error of the mean.

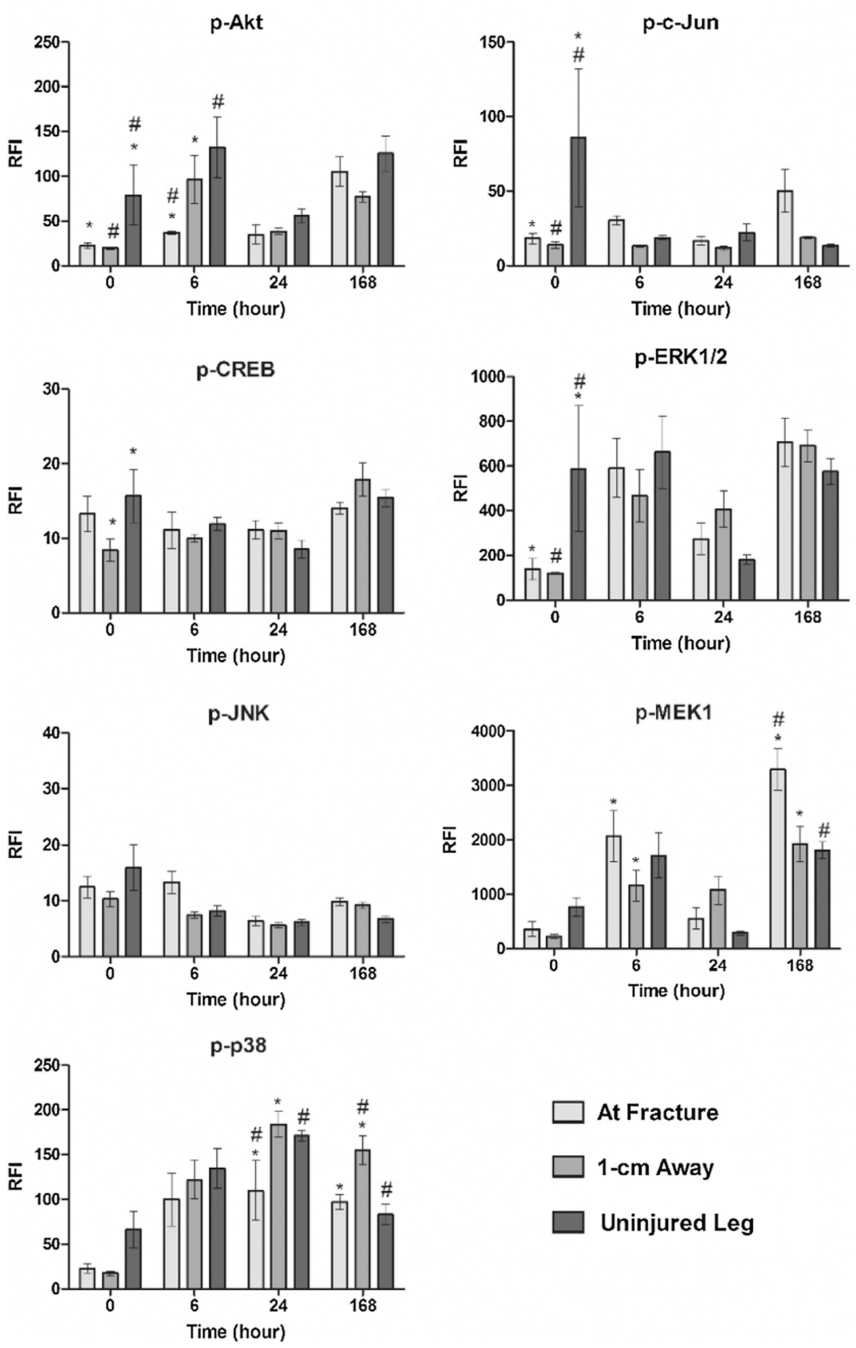

Fig. 2.

Phosphorylation levels measured across time and location in response to a traumatic injury. Levels of phosphorylated protein of Akt, c-Jun, CREB, ERK1/2, JNK, MEK1, and p38 were determined for each time point and location. Concentrations are expressed as relative fluorescence intensity (RFI). Statistically significant differences ($p < 0.05$) in protein concentration between different locations are marked with matching symbols (* or #). Error bars reflect ± standard error of the mean.

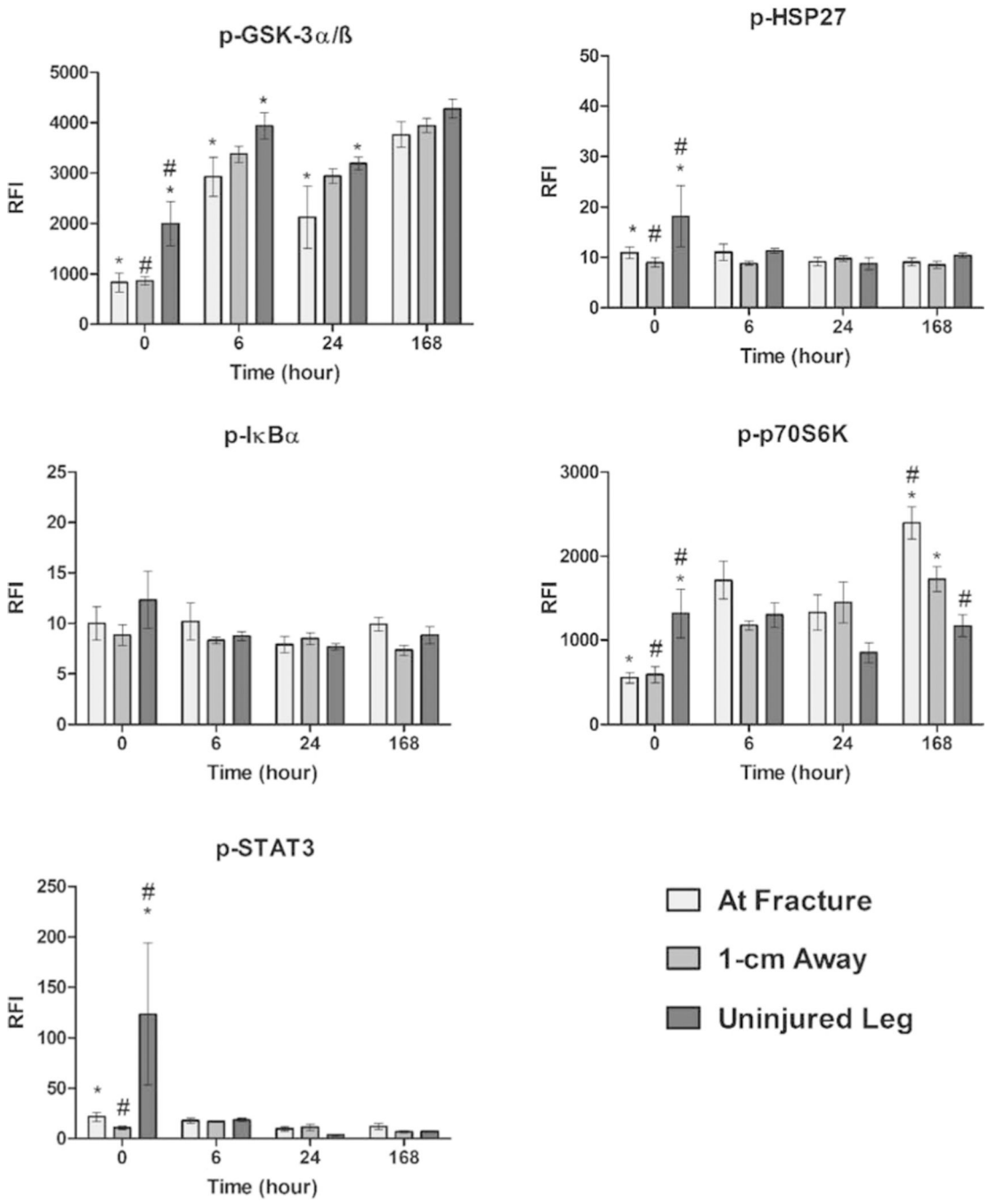

Fig. 3.

Phosphorylation levels measured across time and location in response to a traumatic injury. Levels of phosphorylated protein of GSK-3α/ß, HSP27, IκBα, p70S6K, STAT3 were determined for each time point and location. Concentrations are expressed as relative fluorescence intensity (RFI). Statistically significant differences ($p < 0.05$) in protein concentration between different locations are marked with matching symbols (* or #). Error bars reflect ± standard error of the mean.

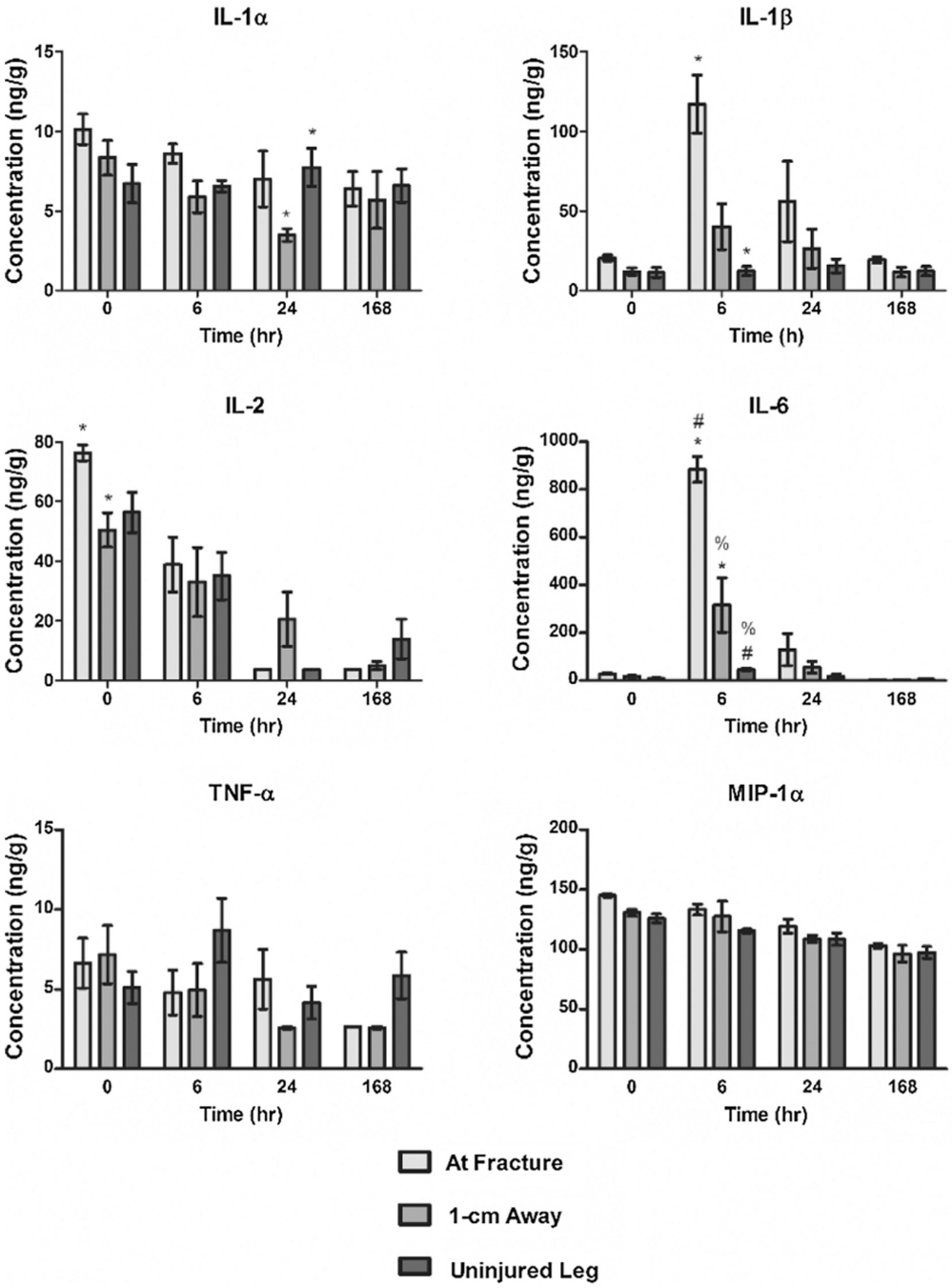

Fig. 4.

Cytokine levels measured across time and location in response to a traumatic injury. Concentrations (ng/g) of IL-1α, IL-1ß, IL2, IL6, TNF-α, and MIP-1α were determined for each time point and location. Statistically significant differences ($p < 0.05$) of cytokine concentration between different locations at each time point are marked with matching symbols (*, #, or %). Error bars reflect ± standard error of the mean. Figure reprinted from Cytokine, 66, H.N. Currie, M.S. Loos, J.A. Vrana, K. Dragan, J.W. Boyd, Spatial cytokine

distribution following traumatic injury, 112–118, Copyright 2014, with permission from Elsevier.

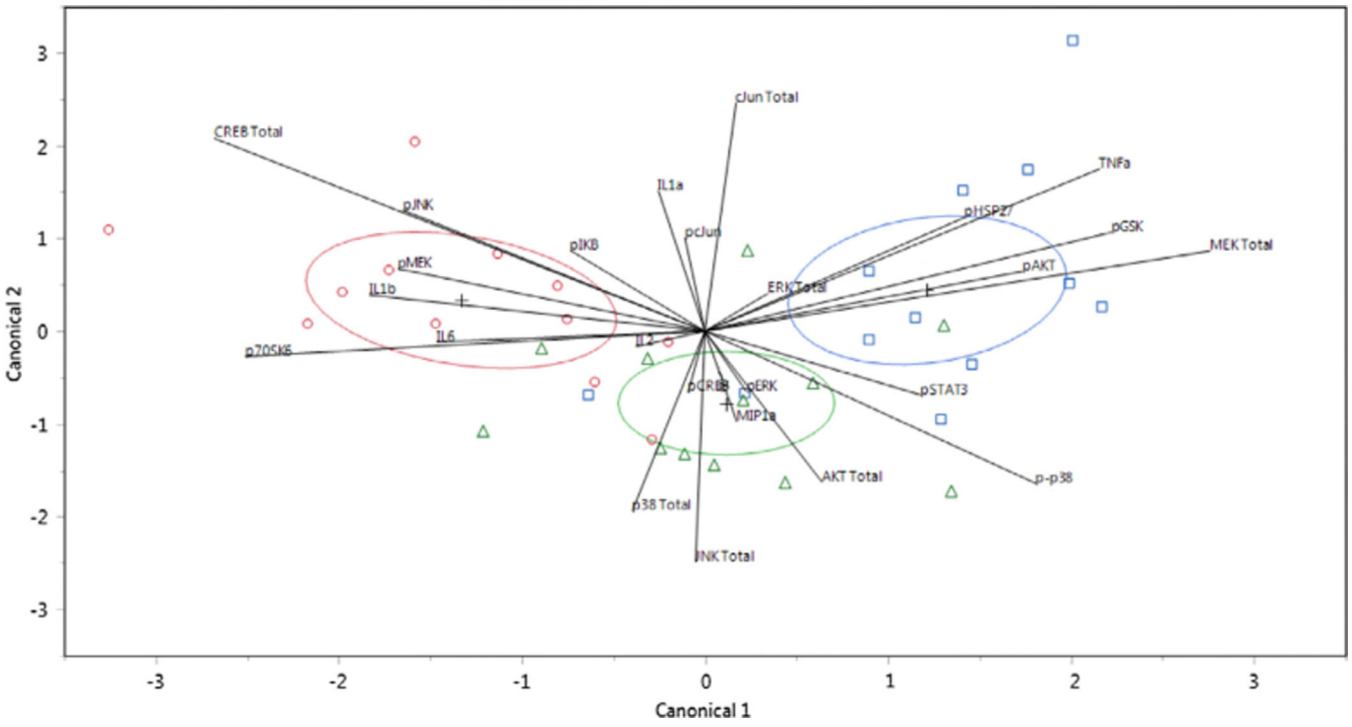

Fig. 5.

Canonical scores plot for the identification of the location of injury. Canonical scores for each covariate calculated by quadratic discriminant analysis are plotted. The different locations of injury, at the site (red circles), 1-cm away (green triangles), and on the other uninjured leg (blue squares), were identified. The + signifies the mean of the covariates in each group. The ellipses represents a 95% confidence level and the biplot rays describe the degree of association of a certain covariate with the canonical variables. (For interpretation of the references to color in this figure legend, the reader is referred to the web version of this article.)

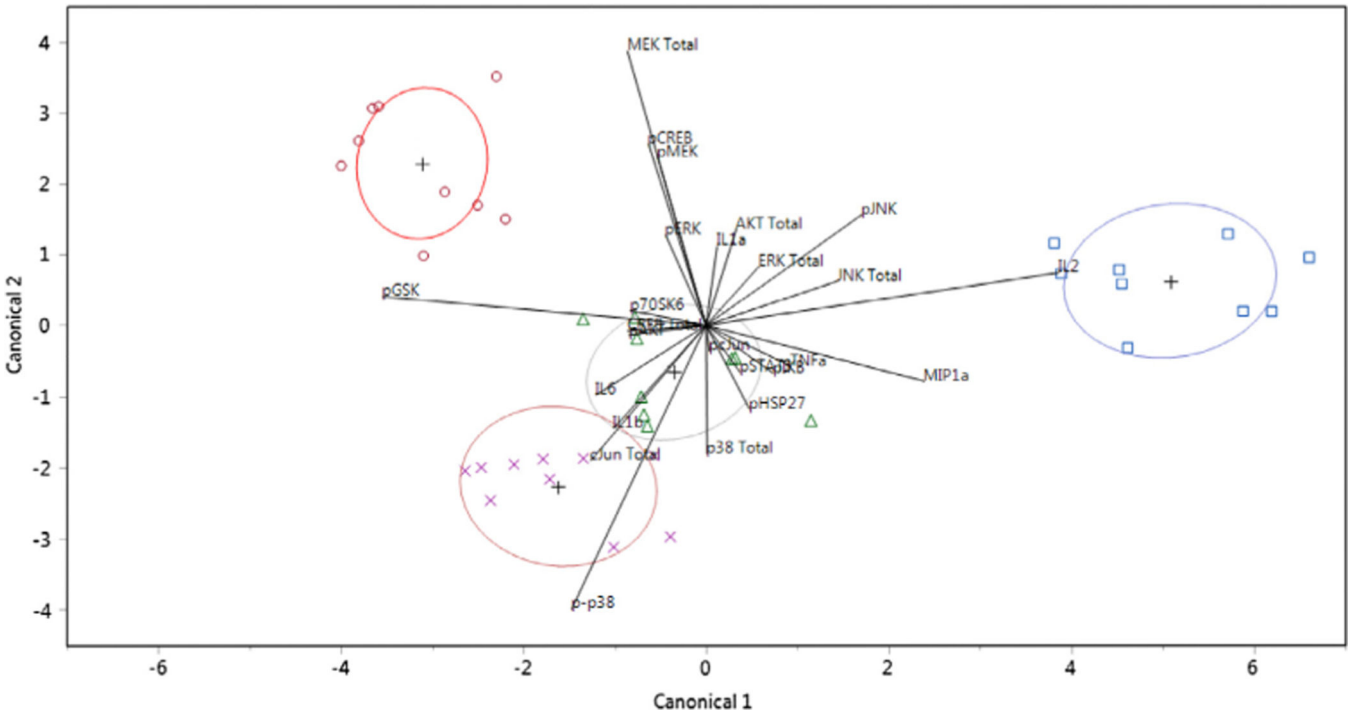

Fig. 6.

Canonical scores plot for the identification of the time of injury. Canonical scores for each covariate calculated by quadratic discriminant analysis are plotted. The different times of injury, 0 (blue squares), 6 (green triangles), 24 (purple X's) and 168 (red circles) h were identified. The + signifies the mean of the covariates in each group. The ellipses represents a 95% confidence level and the biplot rays describe the degree of association of a certain covariate with the canonical variables. (For interpretation of the references to color in this figure legend, the reader is referred to the web version of this article.)

Table 1

Results of spatial cytokine-total protein response correlation analysis. Pearson correlation coefficients (*r*) and significance values (*p*) for associated cytokines and total protein levels across all sampling locations are listed. *N*=12 and any outliers driving correlations were identified and removed.

Cytokine	Total protein	Correlation (*r*)	*p*
At fracture			
MIP-1α	CREB	−0.7570	0.0112
MIP-1α	MEK1	−0.7740	0.0086
MIP-1α	c-Jun	−0.7447	0.0135
MIP-1α	Akt	−0.6485	0.0425
IL2	MEK1	−0.7521	0.0121
TNF-α	MEK1	−0.7728	0.0088
IL-1α	MEK1	−0.6630	0.0367
IL-1α	JNK	−0.6302	0.0377
IL-1β	ERK1/2	−0.6498	0.0420
1-cm Away			
MIP-1α	CREB	−0.7023	0.0109
MIP-1α	p38	−0.5849	0.0458
IL2	CREB	−0.7846	0.0025
IL2	Akt	−0.5873	0.0447
Uninjured leg			
IL6	MEK1	−0.7139	0.0091
IL2	MEK1	−0.5944	0.0415
IL-1α	Akt	0.6174	0.043

Table 2

Results of spatial cytokine-phosphorylated protein response correlation analysis. Pearson correlation coefficients (*r*) and significance values (*p*) for associated cytokines and phosphorylation responses across all sampling locations are listed. $N = 12$ and any outliers driving correlations were identified and removed.

Cytokine	Phosphoprotein	Correlation (*r*)	*P*
At fracture			
MIP-1α	p-Akt	−0.8639	0.0013
MIP-1α	p-p70S6	−0.8297	0.0016
MIP-1α	p-GSK-3α/β	−0.8161	0.0022
MIP-1α	p-MEK1	−0.6863	0.0197
MIP-1α	p-ERK1/2	−0.6515	0.0299
1-cm Away			
MIP-1α	p-Akt	−0.6449	0.0321
MIP-1α	p-GSK-3α/β	−0.5807	0.0477
IL2	p-p70S6	−0.7543	0.0046
IL2	p-Akt	−0.7547	0.0073
IL2	p-IκBα	0.6273	0.0388
IL2	p-GSK-3α/β	−0.5913	0.0429
IL-1β	p-STAT3	0.7341	0.0066
Uninjured leg			
IL2	p-STAT3	0.6633	0.0261
IL2	p-JNK	0.6416	0.0333
TNFα	p-ERK1/2	0.8460	0.0005
TNFα	p-p70S6	0.7598	0.0041

Table 3

Results of temporal cytokine-total protein response correlation analysis. Pearson correlation coefficients (*r*) and significance values (*p*) for associated cytokines and total protein levels across all time points are listed. *N* =9 and any outliers driving correlations were identified and removed.

Cytokine	Total protein	Correlation (*r*)	*P*
T = 0			
IL6	p38	−0.7923	0.0109
IL6	c-Jun	−0.8543	0.0144
IL6	MEK1	−0.6888	0.0402
IL-1α	c-Jun	−0.8885	0.0075
TNFα	p38	−0.7761	0.0139
IL2	p38	−0.7291	0.0258
IL2	MEK1	−0.7252	0.0270
MIP-1α	c-Jun	−0.8098	0.0273
T = 6			
IL6	p38	−0.8690	0.0024
IL6	ERK1/2	−0.8733	0.0046
IL6	JNK	−0.8410	0.0089
IL-1β	p38	−0.8507	0.0036
IL-1β	JNK	−0.8225	0.0122
IL-1β	ERK1/2	−0.8865	0.0033
T=24	No correlations		
T=168	No correlations		

Table 4

Results of temporal cytokine-phosphorylated protein response correlation analysis. Pearson correlation coefficients (*r*) and significance values (*p*) for associated cytokines and phosphorylation responses across all time points are listed. $N = 9$ and any outliers driving correlations were identified and removed.

Cytokine	Phosphoprotein	Correlation (*r*)	*P*
T = 0			
IL-1α	p-GSK-3α/β	−0.7709	0.0251
IL-1α	p-p70S6	−0.7538	0.0308
IL6	p-CREB	0.7121	0.0314
IL2	p-CREB	0.6966	0.0371
IL2	p-MEK1	0.6834	0.0424
T = 6			
IL-1α	p-c-Jun	0.8207	0.0125
IL-1β	p-JNK	0.7943	0.0186
MIP-1α	p-Akt	−0.7101	0.0484
T = 24			
IL6	p-HSP27	0.9184	0.0035
IL6	p-CREB	0.7892	0.0349
IL-1β	p-HSP27	0.8060	0.0286
T = 168	No correlations		